Separation Science and Technology
Publication details, including instructions for authors and subscription information:
http://www.informaworld.com/smpp/title~content=t713708471

Pulse-injection studies of blood progenitor cells in a quadrupole magnet flow sorter

Mauricio Hoyos[a]; Kara E. McCloskey[b]; Lee R. Moore[b]; Masayuki Nakamura[b]; Brian J. Bolwell[c]; Jeffrey J. Chalmers[d]; Maciej Zborowski[e]
[a] Ecole Supérieure de Physique et Chimie Industrielles, Paris, France [b] Department of Biomedical Engineering, The Cleveland Clinic Foundation, Cleveland, OH, U.S.A. [c] Department of Biomedical Engineering, The Taussig Cancer Center, The Cleveland Clinic Foundation, Cleveland, OH, U.S.A. [d] Department of Chemical Engineering, 121 Koffolt Laboratories 140 West 19th Avenue, The Ohio State University, Columbus, OH, U.S.A. [e] Department of Biomedical Engineering,

Online publication date: 23 April 2002

To cite this Article Hoyos, Mauricio , McCloskey, Kara E. , Moore, Lee R. , Nakamura, Masayuki , Bolwell, Brian J. , Chalmers, Jeffrey J. and Zborowski, Maciej(2002) 'Pulse-injection studies of blood progenitor cells in a quadrupole magnet flow sorter', Separation Science and Technology, 37: 4, 745 — 767
To link to this Article: DOI: 10.1081/SS-120002215
URL: http://dx.doi.org/10.1081/SS-120002215

SEPARATION SCIENCE AND TECHNOLOGY, 37(4), 745–767 (2002)

PULSE-INJECTION STUDIES OF BLOOD PROGENITOR CELLS IN A QUADRUPOLE MAGNET FLOW SORTER

Mauricio Hoyos,[1,2] Kara E. McCloskey,[2,4] Lee R. Moore,[2] Masayuki Nakamura,[3] Brian J. Bolwell,[2,3] Jeffrey J. Chalmers,[4] and Maciej Zborowski[2,*]

[1]Laboratoire de Physique et Mécanique des Milieux Hétérogènes, Ecole Supérieure de Physique et Chimie Industrielles, UMR 7636 CNRS, Paris, France
[2]Department of Biomedical Engineering and
[3]The Taussig Cancer Center, The Cleveland Clinic Foundation, 9500 Euclid Avenue, Cleveland, OH 44195
[4]Department of Chemical Engineering, 121 Koffolt Laboratories, The Ohio State University, 140 West 19th Avenue, Columbus, OH 43210-1180

ABSTRACT

A continuous flow, magnetic separation method has been proposed to isolate large numbers of cells for clinical and biotechnological applications. The separation system, based on the quadrupole magnet flow sorter, has been tested on magnetically labeled, human blood progenitor cells using monoclonal antibody against the cluster of differentiation 34 (CD34) molecule and a magnetic colloid. A small volume of the cell suspension was injected into the sorter at variable volumetric flow rates, and the resulting cell elution profiles

*Corresponding author. Fax: (216) 444-9198; E-mail: zborow@bme.ri.ccf.org

were analyzed for cell recovery in the magnetically enriched and depleted cell fractions. Independently, the cell motion in the magnetic field has been analyzed using a novel technique of cell tracking velocimetry, which allowed the determination of cell magnetophoretic mobility. A mathematical model of the cell motion inside the quadrupole flow sorter was used to calculate the recovery of the sorted fractions based on the cell magnetophoretic mobility distribution. A comparison of experimental and theoretical data allowed the verification of assumptions underlying the magnetic cell separation process, and provided guidelines for engineering design of the magnetic flow sorter.

INTRODUCTION

Cell separation plays an important role in the biomedical sciences and in clinical therapy. Cell-separation methods have progressed considerably during the past few decades due to the increasing demand for high-quality cell products. The current applications of the cell products require high purity, high recovery, and high speed of the cell separation process (1). Density gradient centrifugation remains a mainstay of bulk cell-separation applications such as the fractionation of blood into cellular and liquid (plasma) components, as well as sub-fractionation of white blood cell populations (2). Continuous centrifuges are used routinely for clinical apheresis procedures, during which various fractions of blood such as platelets or white blood cells are collected from patients on-line and the remainder of the blood is returned to the patient (3). Immunoaffinity columns have been proposed to engineer the composition of the bone marrow or the apheresis product for cellular therapies of cancer (4). Highly-specialized fluorescence-activated cell sorters (FACSs) play a fundamental role in expanding our understanding of the cell function and the properties of the human immune system at a cellular level (5).

Magnetic cell separation methods have seen a rapid development, particularly in the last decade (6–14). The advantages of magnetic separation include its relative simplicity of operation, versatility, and relatively low capital and operating costs. The biomedical applications of magnetic separation extend from molecular biology to clinical cellular therapy. In particular, cellular therapy based on the magnetic separation of hematopoietic (blood-forming) progenitor cells appears to be a promising approach for the treatment of cancer and gene therapy (3,4,11).

The interaction of a cell with a magnetic field is usually mediated by a magnetic particle conjugated to a chemical reagent, which reacts specifically with the targeted cell population. In simple terms, the specificity of the magnetic cell

MARCEL DEKKER, INC.
270 Madison Avenue, New York, New York 10016

separation is determined by the specificity of the targeting reagent, whereas its sensitivity is determined by the amount of magnetization imparted to a cell by the magnetic particle. In practice, the purity and recovery of the sorted cell fractions depend not only on the properties of the magnetizing reagent but also on the design of the magnetic separator (12,14,15). Large magnetic particles, in the diameter range 150 nm–5 μm, produce a large magnetic moment when placed in a moderate magnetic field, and thus are used typically in combination with open gradient magnetic fields, such as those produced by small permanent magnets, placed outside the cell suspension container (10,15). Small magnetic particles, in the diameter range 12–100 nm, produce a small magnetic moment and therefore require the use of high-gradient magnetic separation (HGMS) fields, such as those produced by thin wires of a ferromagnetic material immersed in the cell suspension (6–9,11).

Currently, magnetic cell separators operate in batch mode, and they are difficult to scale up and stage. Moreover, magnetic batch separators do not allow for quantitative magnetic cell fractionation in which the cell population is fractionated according to the amount of the magnetic reagent attached to the cell. Quantitative cell fractionation may become important for cell function studies and for early progenitor cell isolation. Therefore, we have proposed to extend the magnetic separation methods to a continuous system based on an open gradient, quadrupole magnetic field geometry and an annular flow channel (12,13,16). The expected advantages of such a system include flexibility in scale-up and staging of the separation process, as well as the potential for a quantitative cell fractionation based on the cell surface marker expression (17,18). The properties of the quadrupole magnetic flow sorter (QMS) system have been studied theoretically and experimentally (13,16,18). In particular, we have investigated the relationship between the cell magnetophoretic mobility, and the purity, recovery, and throughput of the sorted cell fractions. The cell magnetophoretic mobility has been defined by analogy to the cell electrophoretic mobility (used in free-flow cell electrophoresis) as a ratio of the field-induced cell velocity to the strength of the magnetic force, S_m (19–23). Cell separation results from differences in cell magnetophoretic mobilities in the continuous QMS system. The concept of the cell magnetophoretic mobility allows the separation of variables describing properties of the cell from those of the external magnetic field. Provided that the magnetically labeled cluster of differentiation 34 (CD34) cell behaves as an ideal, induced magnetic dipole, the magnetophoretic mobility of the cell, m, depends on the binding of the antibody to the cell and the magnetic susceptibility of the magnetic label, but not on the external magnetic field (17). In turn, the magnetic force strength, S_m, depends on the field strength of the source and the field geometry, but is independent of the cell (and the magnetic label) properties (14). Such a separation of variables simplifies the theoretical and experimental treatment of the continuous cell

MARCEL DEKKER, INC.
270 Madison Avenue, New York, New York 10016

sorting process greatly, and is the basis of the cell sorting process analysis described in this work.

Magnetophoretic mobilities of the cell populations were measured using cell tracking velocimetry (CTV) (23,24). The theory of QMS operation was developed on the basis of the theory of the split-flow thin (SPLITT) fractionation (18), developed by Giddings and co-workers (25). Experimental verification was performed using CTV and continuous separation experiments with reference magnetic bead standards and white blood cells (13,16). The goal of the current work is to extend the experimental work to hematopoietic progenitor cells. We elected to work on a pure progenitor cell population in order to simplify the system performance analysis. The long-term goals of this study are to understand the mechanics of the continuous magnetic cell separation process better and to develop a conceptual framework necessary for the design engineering of a clinical QMS prototype.

MATERIALS AND METHODS

The Cell Model System

The source of the hematopoietic progenitor cells for QMS experiments was the white blood cell fraction from patients undergoing clinical apheresis and autologous blood progenitor cell transplantation, as an adjunct therapy of cancer. As a part of the clinical therapy protocol, the patients underwent progenitor cell mobilization to increase the number of the circulating progenitor cells (3). The use of human material for this study was approved by the Institutional Review Board, and patients participating in this study signed a consent form. The identity of the patients was not recorded for this study, and the sample material was destroyed at the completion of the experiment. The cells from a single patient were used in this study to eliminate patient-to-patient variability in the progenitor cell characteristics as a potential source of error.

A 15 mL sample of the apheresis product containing approximately $(2-3) \times 10^9$ mononuclear cells was washed with a buffer comprising 0.5% (w/v) bovine serum albumin (BSA) and 2 *mM* ethylenediamine tetraacetate (EDTA) in Ca- and Mg-free phosphate-buffered saline (PBS). The PBS composition was 137 *mM* NaCl, 2.7 *mM* KCl, and 10 *mM* dibasic sodium phosphate in distilled water, pH 7.3–7.5 at 25°C (prepared from 10 × concentrate, PBS Liquid Concentrate, EM Science, Merck KGaA, Darmstadt, Germany). The total cell concentration was determined with a Coulter Z-1 particle counter (Beckman-Coulter, Fullerton, CA). Seven hundred million cells were used in the experiment. A CD34 was used as the distinguishing cell surface molecule of

MARCEL DEKKER, INC.
270 Madison Avenue, New York, New York 10016

human blood progenitor cells (26,27). Blood progenitor cells were labeled sequentially with FcR blocking reagent to inhibit nonspecific antibody binding, anti-CD34 (QBEND/10) antibody conjugated to a hapten, and anti-hapten magnetic nanospheres (MACS™ CD34 Progenitor Cell Isolation kit, Miltenyi Biotec, Auburn, CA; additional information about the kit and the MACS separation process is provided at the company website, http://www.miltenyibiotec.com). The nominal diameter of the MACS nanospheres is 50 nm. The cells were washed to remove the unbound reagent from the solution, and the total cell concentration was adjusted to 200 million/mL. Aliquots of 1 mL were pipetted onto MiniMACS column (Miltenyi Biotec), and three sequential isolations and three columns (such that the positive eluent from one column was used as a feed for the next column) were used to achieve high progenitor cell purity. The column was washed three times with 1 mL buffer aliquots to remove the unlabeled cells, which were discarded subsequently. The column was removed from the MiniMACS magnet, and after the addition of 1 mL buffer the contents were flushed out with a plunger and collected as the CD34-positive cell fraction. The three CD34 cell fractions were combined, diluted to approximately 15 mL, and counted. Approximately 10% of this volume was used for the CTV analysis, the rest was used for the QMS separation, as described below. The purity of the progenitor cells was determined by labeling the final cell mixture with the anti-CD34 (HPCA-2) antibody conjugated to fluorescein isothiocynate (FITC), and by flow cytometry analysis (FACS, FACScan, Becton-Dickinson, San Jose, CA). The CD34 positive cell purity was defined as the ratio of CD34-positive cell number to the total cell number in the sample.

The Cell Magnetophoretic Mobility Measurement by Cell Tracking Velocimetry

By analogy to the term "cell electrophoretic mobility" describing the motion of the cell in a suspension exposed to an external electric field, we adopted the term "cell magnetophoretic mobility" to describe the motion of the magnetically labeled CD34 cell in an external magnetic field (18–23). The measurement of cell electrophoretic mobility has been considered in the past for potential diagnostic applications, and has been used for predicting the performance of free-flow cell electrophoresis, a continuous cell separation technique based on an electrostatic field (19,21). The cell magnetophoretic mobility plays an analogous role to the cell electrophoretic mobility when applied to the magnetostatic fields.

The velocity of a magnetically labeled cell induced by the magnetic field is expressed as a product of its magnetophoretic mobility, m, and the local force

MARCEL DEKKER, INC.
270 Madison Avenue, New York, New York 10016

field strength, S_m:

$$u_m = mS_m \tag{1}$$

The force field strength has been defined as follows:

$$S_m = \left|\nabla\left(\frac{B^2}{2\mu_0}\right)\right| \tag{2}$$

where the straight brackets, $|\cdot|$, denote the magnitude of the vector, B the magnetic induction (or the magnetic flux density), μ_0 the magnetic permeability of vacuum, and $\nabla = [\partial/\partial x, \partial/\partial y, \partial/\partial z]$ is a nabla (or del) operator, producing a gradient when operating on a scalar quantity (14). The force field strength, as defined here, has the dimensions of T A/m^2, which is equivalent to N/m^3 (force density); the magnetophoretic mobility has the dimensions of m^3/(T A sec), where N is the unit of force (Newton), T the unit of the magnetic field induction (Tesla, equal to 10,000 G, or Gauss), A the unit of the electric current intensity (ampere), and m and sec have the usual meaning of the units of length and time (meter and second, respectively).

The magnetophoretic mobilities of the CD34 cells labeled with the magnetic colloid were measured using CTV. The CTV technique allows an automated motion analysis of hundreds to thousands of cells to be exposed to a magnetic field (23,24). The unique feature of the CTV instrument developed in our laboratories is that S_m = constant, which improves the accuracy and the resolution of the method significantly. The description of the CTV technique is provided in our earlier publications (17,22–24) and is summarized below.

Briefly, the CD34 cells used for the CTV analysis were suspended in a wash buffer (as described above) with particular care given to obtaining a single-cell suspension (no cell aggregates in the suspension). The cell number concentration was adjusted to 2×10^6/mL approximately. The velocity of the particles in solution was measured in an external magnetic field generating a force field strength of $S_m = 198\,\mathrm{T\,A/mm^2}$, which was nearly constant for the entire field of observation (5× objective). The images of the moving particles were acquired by a CCD camera (CCD 4915, Cohu, San Diego, CA) mounted on a microscope and analyzed by the CTV software (developed and owned by the Ohio State University) running on an IBM-compatible PC with an image board (μ-Tech Vision 1000 PCI Bus Frame Grabber, MuTech Corp., Billerica, MA). Typically, the motion of several hundred cells was analyzed and displayed in the form of the magnetophoretic mobility histograms. The CTV output provided us with the statistics of the CD34 cell samples, such as the magnetophoretic mobility frequency histograms, average mobilities, and the standard deviations.

The experimentally measured distribution of magnetophoretic mobilities was used as an input for a computer program developed to calculate the CD34 cell number concentration distribution in the QMS separator and to predict the expected CD34 cell retrieval factors. The following assumptions were made in calculating the cell concentration inside the QMS separator: the magnetically labeled cells behave as point-like particles; no inter-particle interactions; perfect field and flow geometries; magnetic and viscous forces only; no fringing fields at the ends of the QMS separation element. The resulting cell number distribution between the outlets a and b (and the outer cylinder wall, w) provided a theoretical prediction of the QMS performance, verifiable by the QMS separation experiments, as described below.

The Quadrupole Magnetic Flow Sorter System

The separation element of the QMS separator consisted of two concentric cylinders (the inside cylinder was solid) surrounded by four pole pieces generating the magnetic quadrupole field, as shown in Fig. 1. Quadrupole magnetic flow sorter inlets and outlets were connected to the QMS separation area by suitable flow manifolds, equipped with an inlet and outlet flow splitters, respectively. The source of the magnetomotive force were four pieces of neodymium–iron–boron (Nd–Fe–B) permanent magnets. The quadrupole field geometry was achieved by using four, specially shaped soft iron pole pieces connected to the permanent magnets. The magnetic force field strength, S_m, inside the quadrupole field is axially symmetric:

$$S_m = \frac{B_0^2}{\mu_0 r_o}\rho \tag{3}$$

where $\rho = r/r_o$ is the dimensionless radial distance from the quadrupole field axis, r the distance from the field axis, r_o the outer cylinder inner wall radius, and B_0 the magnetic field at the outer cylinder inner wall (at $\rho = 1$). Note that the force field strength inside the quadrupole field has a centrifugal character, i.e., it is a linear function of the distance from the field's axis of symmetry. There are no tangential or axial components of the force strength inside an ideal quadrupole field (Fig. 1). Our previous work with the magnetic reference beads and other types of cells indicated that indeed, in a close-to-ideal quadrupole field, the radial component of the force dominates (12). The quadrupole magnet's aperture, its length, and the dimensions of the flow channel are shown in Table 1. The characteristic magnetic field parameters, B_0, and the mean force field strength, S_m, are also included in Table 1. The details of the magnetic field geometry inside the separation element of the QMS channel were published elsewhere (12,13).

MARCEL DEKKER, INC.
270 Madison Avenue, New York, New York 10016

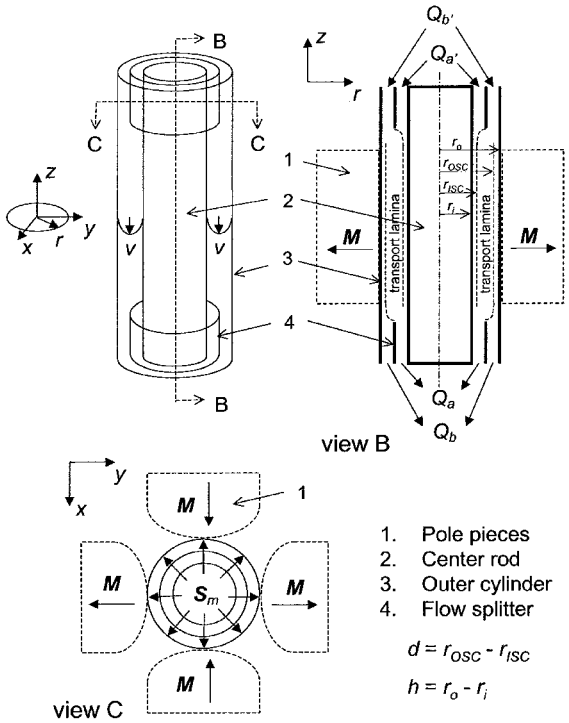

Figure 1. Perspective and cross-section views of the QMS separation element. The QMS separation element was placed outside the magnet for the control experiments (field not acting) and inside the magnet for the test experiments (field acting). In the perspective view, the magnetic pole pieces are not shown for clarity (field off configuration). Note the flow velocity profile, v. Note positions of the four magnetic pole pieces in cross-sectional views, and the radial disposition of the magnetic force field strength, S_m. The cell sample was injected into substream $Q_{a'}$, the carrier medium into substream $Q_{b'}$, and the sorted fractions were collected in substreams Q_a (nonmagnetic) and Q_b (magnetic).

The magnetic field in the QMS separation element is the source of the radial movement of the magnetically labeled cell:

$$u_m = mS_m = m\frac{B_0^2}{\mu_0 r_o}\rho \tag{4}$$

where the cell velocity induced by the magnetic field, u_m, was obtained by combining Eqs. (1) and (3). Because of the distributed character of the CD34 cell magnetophoretic mobility, m, the radial cell velocity, u_m, was also distributed for any given ρ in the magnetic field accessible to cells. Therefore, in calculating the

Table 1. The Quadrupole Magnet Flow Sorter (QMS) System Parameters

Parameter	Value
Maximum field, B_0 (T, tesla)	1.344
Maximum energy product of permanent magnets (MGOe $= 10^6$ Gauss Oersted)	40
Bore (aperture) radius (mm)	4.82
Force field strength, S_m (T A/mm^2)	198
Magnet length, L, (equal to the QMS separation element length) (mm)	76.2
Outer cylinder radius, r_o (mm)	4.53
Inner rod radius, r_i (mm)	2.38
Channel height, h (mm)	2.15
Void volume of the QMS flow channel (mL)	6.3
Inlet flow splitter radius (mm)	3.12
Outlet flow splitter radius (mm)	3.54
Inlet flow rate ratio, $Q_{a'}/Q$	0.1
Outlet flow rate ratio, Q_a/Q	0.2
Total flow rate, Q (mL/min)	2,3,4,5,6,7,8,10,12,15

retrieval factors at outlets a and b, we used sets of trajectories corresponding to different mobilities, with weighting factors equal to the mobility frequency as measured by the CTV. An additional source of the distribution of the cells between the outlets a and b was the random distribution of cell initial radial position when entering the magnetic field region. The combination of the radial (magnetic) and axial (convective) velocity components determined the final position of the cell in the fluid stream at the outlet flow splitter, and therefore the cell assignment to either outlet a or b.

The elution of the CD34 cells from the QMS separator following a pulse injection was studied using the experimental setup shown in Fig. 2. The cell sample was injected into inlet a′ and the carrier was pumped into inlet b′, while the magnetically labeled CD34 cell fraction was collected at outlet b and the rest of the cells exited through outlet a. The fractional flow rates $Q_{a'}$, $Q_{b'}$, Q_a, and Q_b were controlled using two dual-syringe pumps (Type 33 syringe pump, Harvard Instruments, Inc., Natick, MA), one set to injection ($Q_{a'}$, $Q_{b'}$), the other to aspiration (Q_b) mode, such that $Q_{a'} + Q_{b'} = Q_a + Q_b = Q$. The volumes of the syringes (Becton-Dickinson, Franklin Lakes, NJ) a′, b′, and a used for pumping the carrier fluid were: 30, 140, and 140 mL, respectively. Outlet b was left open to the atmosphere to equilibrate the pressure. A teflon tubing of 0.8 mm internal diameter was used for fluid connections. A six-way valve with a 50-μL sample loop (Rheodyne 7725i, Alltech Associates, Inc., Deerfield, IL) was used for pulse

MARCEL DEKKER, INC.
270 Madison Avenue, New York, New York 10016

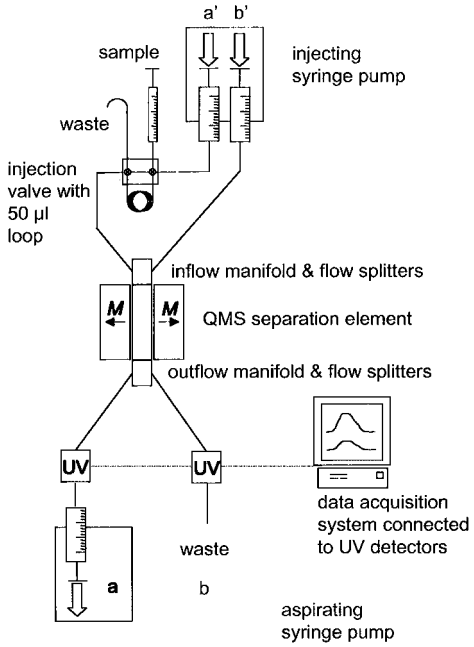

Figure 2. The block diagram of the QMS pulse injection system.

injection of the magnetic cell suspensions into the a′ substream. Outlets a and b of the QMS separator were connected to two 254 nm UV detectors with 32 μL flow cells (VUV-10, HyperQuan, Inc., Colorado Springs, CO). The detector signal was fed into an analog-to-digital converter (DI-190, Dataq Instruments, Akron, OH) and stored in an IBM-compatible PC. The data were displayed and recorded using a software package (WinDaq Lite, Dataq Instruments), and analyzed with a specialized software for peak deconvolution and parameterization (PeakFit, SPSS, Inc., Chicago, IL). The pulse of a small volume of the cell suspension applied to the inlet of the QMS separator (at the inlet a′) produced pulses of increased light attenuation at the outlets a and b, characteristic of the distribution of the eluted fractions between outlets a and b, respectively. The correlation of the light attenuation peaks with the volume fraction of cells crossing the UV detector led to an accurate and direct determination of the cell retrieval factors in outlets a and b.

The inlet flow rate ratio, Q_a'/Q, and the outlet flow rate ratio, Q_a/Q, determined the positions of the flow stream surfaces originating at the edges of the inlet and outlet flow splitters inside the QMS channel, respectively. These characteristic stream surfaces were referred to as "inlet splitting cylinder" (ISC)

and "outlet splitting cylinder" (OSC) in analogy to the SPLITT fractionation theory developed by Giddings (18,28). The volume of flow enveloped by the ISC and OSC was referred to as "the transport lamina", and it represented a resistive element to transport during the separation process in the QMS channel (Fig. 1) (16,18,29). The effect of flow imperfections in the QMS system has been observed as a residual cell transport across the transport lamina even in the absence of the magnetic field (dubbed "cell crossover"). The inlet and outlet flow rate ratios for this study were determined by measuring cell crossover on unlabeled (nonmagnetic) cell populations, with the QMS channel outside the magnet.

Prior to the injection of the magnetically labeled CD34 cells, the system was filled with degassed carrier solution consisting of 0.1% Pluronic F-68 in Ca-, Mg-free PBS buffer, with particular attention paid to the removal of air bubbles from the QMS separator and the fluid lines. Both the inlet and outlet flow pumps were started and allowed to run for a few minutes in order to stabilize the flow distribution inside the separator channel. The total and partial flow rates used in the study are indicated in Table 1. A 50 μL cell suspension bolus at a cell number concentration of 5×10^6/mL, was injected into inlet a′ through an injection valve. The development of the elution profiles from the outlets a and b was monitored on the PC screen in real time. The CD34 cell distribution between the outlets a, b, and the outer wall, w, was calculated from the elution profiles, as described below.

Calculation of the CD34 Cell Retrieval Factors from the Pulse-Injection Profiles

The distribution of the CD34 cells between outlets a and b was characterized experimentally by their retrieval factors, F_a and F_b, respectively. The retrieval factor, F_b, of an analyte at outlet b of the separator was defined as the ratio of the number of the CD34 cells eluted at outlet b, N_b, to the number of the CD34 cells injected into the system, N:

$$F_b = \frac{N_b}{N} \tag{5}$$

A similar formula was obtained for the retrieval factor at the outlet a, F_a. The retrieval factor is a measure of the yield or the fractional recovery, of the analyte. The calculation of the number of cells crossing the light path in the detector was based on the observation that the area under the elution profile, A, multiplied by the volumetric flow rate of the cell suspension crossing the detector, Q, is proportional to the total number of cells, N:

$$QA \propto N \tag{6}$$

Marcel Dekker, Inc.
270 Madison Avenue, New York, New York 10016

In order to use the above expression directly for the calculation of the retrieval factors, first a reference QA value was determined by directing the total cell flow through one of the outlets only (say b), with the channel placed outside the magnet. Secondly, the channel was placed inside the magnet, both outlets a and b were opened to the flow, and a new value of the area under the elution profile × the flow rate was determined, Q_bA_b. From Eqs. (5) and (6) one obtains:

$$F_b = \frac{Q_bA_b}{QA} \tag{7}$$

where the subscripted quantities correspond to the normal operation mode of the QMS separator (both a and b outlets open, the flow channel in the magnetic field), and the unsubscripted quantities correspond to the reference operation mode (outlet a closed, the flow channel outside the magnetic field). A similar expression for F_a was obtained for the detector a. The reference A values were determined separately for each detector. In principle:

$$F_a + F_b + F_w = 1 \tag{8}$$

where F_w is the cell fraction retained at the accumulation wall. The fraction F_w was calculated as the difference between $F_a + F_b$ and unity.

RESULTS AND DISCUSSION

The cell sample used for the CTV mobility determination and the QMS separation experiments consisted of blood progenitor cells from patients undergoing stem cell mobilization and clinical apheresis. Following enrichment, the CD34-positive cell content (where CD34 is the blood progenitor cell marker) in the cell samples used in this study was 95%, as measured by FACS flow cytometry (data not shown). The remainder of the cells belonged to a broad category of CD34-negative cells and consisted of a heterogeneous mononuclear cell population.

The magnetophoretic mobility of the blood progenitor cells labeled with the magnetic colloid, m, was measured using the CTV method, and the results are shown in Table 2 and Fig. 3. The cell mobility was distributed over a wide range of almost five orders of magnitude, with the most probable value falling at $1.68 \times 10^{-4}\,\mathrm{mm^3/T\,A\,sec}$, and a 99% confidence interval of $1.59–1.77 \times 10^{-4}\,\mathrm{mm^3/T\,A\,sec}$ ($n = 1000$).

The experimentally measured cell magnetophoretic mobilities (Fig. 3) were used to calculate the CD34 cell retrieval factors at outlets a and b of the QMS, Eq. (5). Examples of cell number concentration distributions for low, optimal, and high flow rates are shown in Fig. 4. Note that at lower flow rates

MARCEL DEKKER, INC.
270 Madison Avenue, New York, New York 10016

Table 2. The CD34 Cell Magnetophoretic Mobility Statistics Generated by the Cell Tracking Velocimetry (CTV) Analytical System (the Corresponding Magnetophoretic Mobility Histogram Is Shown in Fig. 3)

Parameter	Value
Experiment number	266 (ef1)
N ($m > 0$)	1000
Mean mobility, m (mm^3/T A sec)	1.7×10^{-4}
Median m (mm^3/T A sec)	1.53×10^{-4}
Mode m (mm^3/T A sec)	1.68×10^{-4}
Standard deviation of the mean (mm^3/T A sec)	1.1×10^{-4}
99% confidence interval	$1.68 \times 10^{-4} \pm 9.2 \times 10^{-6}$
Coefficient of variation (%)	68
Skewness	5.5
Kurtosis	51.4
Maximum mobility, m (mm^3/T A sec)	1.53×10^{-3}
Minimum mobility, m (mm^3/T A sec)	2.02×10^{-8}
Number of cells with negative mobility, $m < 0$	60
Time between frames (sec)	1/3
Total number of frames used	20

a fraction of cells may contact the outside channel wall before exiting from the magnetic field. Close to the wall, the fluid flow velocity is negligibly small, and therefore the residence time inside the channel for a point-like cell approaching the wall increases to infinity. For calculation purposes, a point-like cell approaching the wall in the magnetic field is treated as if it would be retained inside the channel. This fraction of cells retained inside the channel is described by the wall retrieval factor, F_w, see also Eq. (8). The cells that were retained on the wall were characterized by the highest magnetophoretic mobilities.

The simulated retrieval factors based on the CD34 cell magnetophoretic mobility distribution are shown in Fig. 7. The dependence of F_b on the total flow rate, Q, showed a characteristic maximum: as the total flow rate through the QMS element increased (and the cell residence time in the magnetic field decreased), an increasing number of the CD34 cells were predicted to be directed into outlet b, with a corresponding increase of the parameter F_b. At high flow rates the cell residence time in the magnetic field was not sufficient for the cell to traverse the radial distance separating it from the outlet splitting cylinder and reach the outlet b, with a resulting drop in the retrieval factor F_b. The decrease in transport of cells to outlet b with the increase in total flow rate was accompanied by an increase in the outlet a retrieval factor, F_a, as it should (Fig. 7).

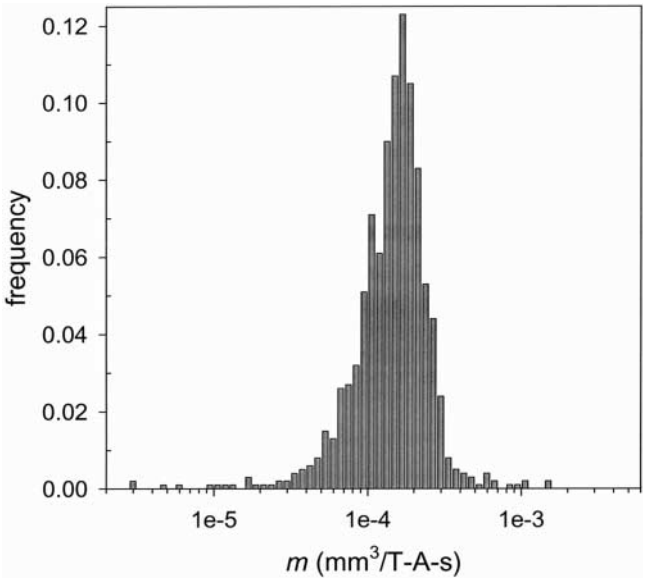

Figure 3. The magnetophoretic mobility distribution of the feed sample. Additional information is provided in Table 2.

The cell mixture containing approximately 95% blood progenitor cells labeled with magnetic colloid was injected into the QMS column, resulting in elution profiles used for the determination of the CD34 cell retrieval factors in outlet a and b. The relationship between the area under the elution curve, the fractional flow rate, and the retrieval factor is given in Eq. (7). An example of typical elution profiles is shown in Fig. 5. Prior to the studies on cell separation in the magnetic field, the effect of possible flow imperfections was minimized by selecting suitable inlet and outlet flow rate ratios, $Q_{a'}/Q$ and Q_a/Q. This was done by analyzing cell crossover outside the magnetic field as a function of transport lamina thickness, d. Characteristically, the cell retrieval factor in outlet b was the highest for $d = 0$ and decreased rapidly with increasing d (Fig. 6). This behavior was attributed to the finite cell size (of the order of 10 μm) and the randomizing effects of flow imperfections, which were the strongest for a transport lamina thickness smaller than 10 cell diameters. During the subsequent CD34 cell separation studies in the magnetic field, $Q_{a'}/Q = 0.1$ and $Q_a/Q = 0.2$ were selected.

The pulse-injection experiments in the magnetic field largely verified the theoretical predictions of the F_b based on the cell magnetophoretic measurements by CTV (Fig. 7). The position of the theoretical and the

MARCEL DEKKER, INC.
270 Madison Avenue, New York, New York 10016

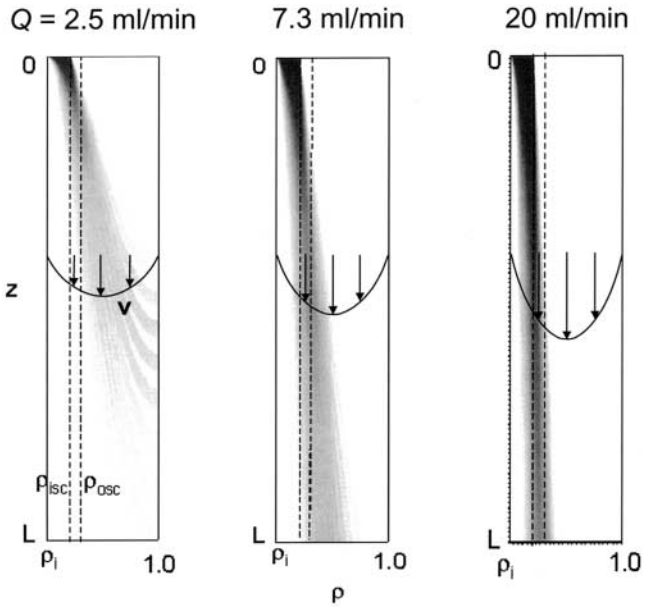

Figure 4. The cell concentration distribution inside the QMS separation element. Note decreasing transport of cells across the transport lamina (between ρ_{ISC} and ρ_{OSC}) with the increasing total flow rate, Q (the direction of flow is from top to bottom; the flow velocity profile, v, is not to scale). The inlet flow rate ratio was $Q_{a'}/Q = 0.1$; the outlet flow rate ratio was $Q_a/Q = 0.2$.

experimental F_b maxima nearly coincided at 7 and 6 mL/min, respectively (Fig. 7). The increase in F_a with Q predicted on the basis of the cell magnetophoretic mobility was verified by the experimentally measured F_a values (Fig. 7). It is worth noting that the computer simulations of the cell retrieval factors, F_a and F_b, were based on the experimentally-determined CTV cell mobility only, independent of the QMS experiments, indicating no need for data fitting. Therefore, we conclude that the agreement between the theoretical results based on the cell mobility measurements by CTV and the observed cell elution patterns from the QMS system, support the basic assumption underlying the cell sorting analysis that the cell magnetophoretic mobility and the strength of the magnetic force field, can be treated as independent variables, Eq. (1).

We observed a consistently higher cell elution in outlet a, and consistently lower elution in outlet b as compared to the theory, at total flow rates equal to or higher than 5 mL/min. The reason for this discrepancy is not clear to us at this time. The possibility exists that this was the result of the presence of unlabeled

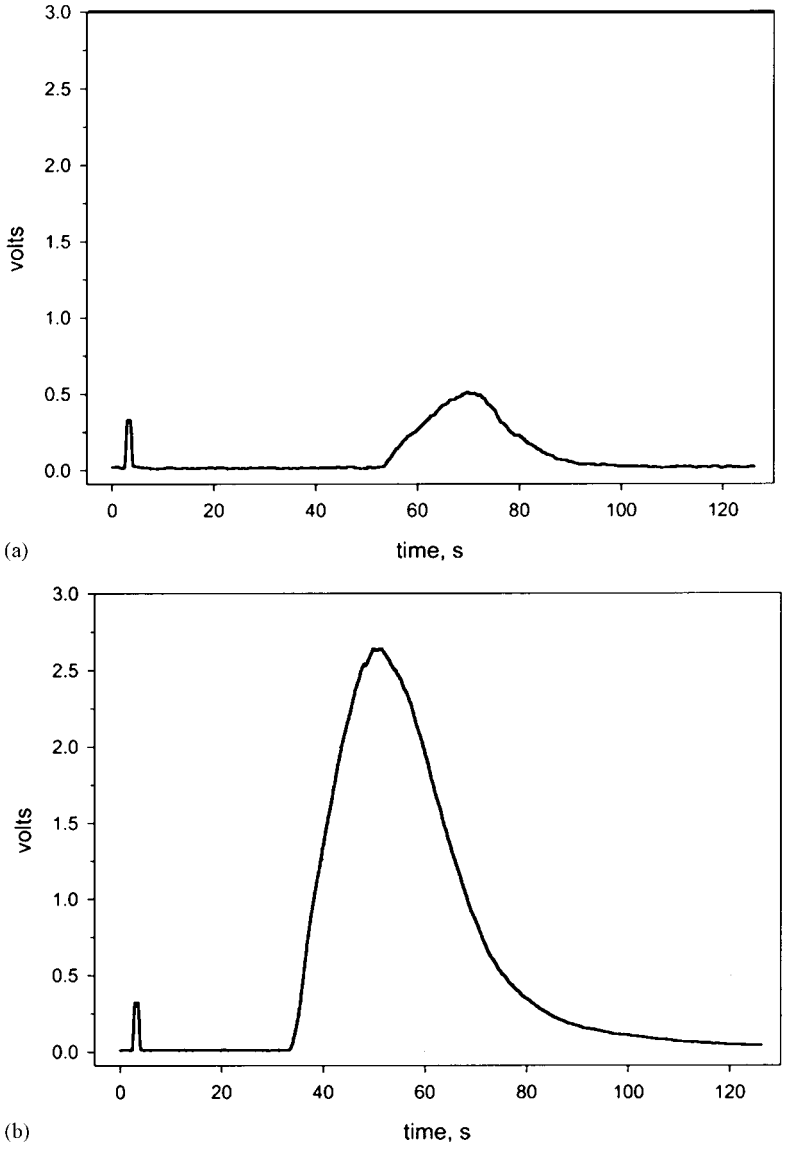

Figure 5. The representative CD34 cell elution profiles: (a) outlet a, (b) outlet b ($Q = 7.0$ mL/min). Note that the b fraction elution time was shorter than that of the a fraction due to the fact that the cells crossing the transport lamina were exposed to the faster-moving flow regions than the cells staying close to the inner cylinder wall.

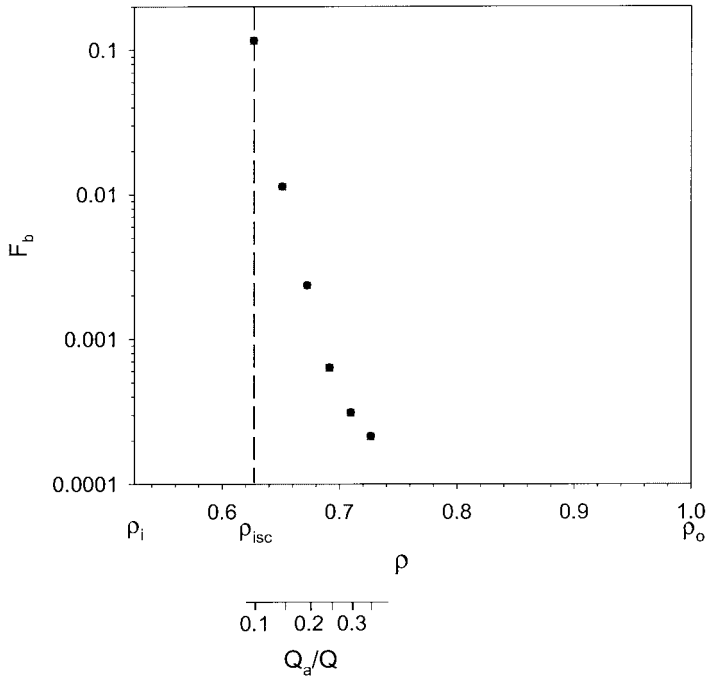

Figure 6. The cell crossover inside the QMS separation element. Note the decrease in transport of cells across the transport lamina (here defined by ρ_{ISC} and the abscissa of an experimental point) with the increase in transport lamina thickness (magnetic field off; $Q = 5\,\text{mL/min}$).

(negative) cell fraction in the mixture. Cell composition analysis by FACS flow cytometry determined that there were approximately 5% of non-CD34 cells in the cell sample, consistent with the lower cell retrieval observed at outlet b and the higher retrieval at outlet a. Moreover, the theory used for the QMS performance prediction was based on assumptions of an infinitesimal cell dimension and the absence of cell–cell interactions, which also may have contributed to the observed differences between the theory and the experiment. The theory may require refinements in order to obtain a better agreement with the experimental results.

The sum of the retrieval factors from outlets a and b, F_a+F_b, was close to that predicted based on the cell magnetophoretic mobility (Fig. 7) within experimental error. The difference between the sum of retrieval factors from both outlets and unity was equal to the cell retention inside the channel, Eq. (8). The

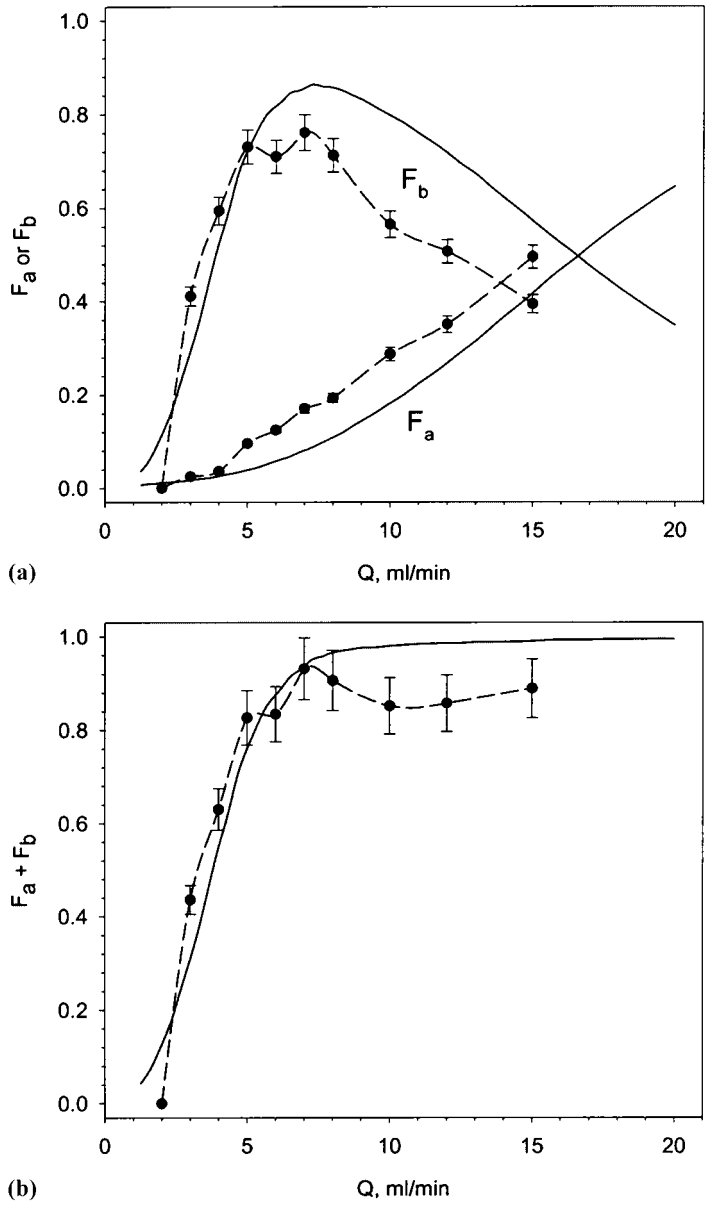

Figure 7. The cell retrieval factors: theory (solid line) and experiment (broken line): (a) outlet a and outlet b; (b) outlet a plus outlet b.

MARCEL DEKKER, INC.
270 Madison Avenue, New York, New York 10016

agreement between the observed and the predicted values of F_a+F_b suggests that the proposed mechanism for cell retention at lower channel flow rate (i.e., migration of the highest mobility cells to the outer wall) is reasonable and sufficient to account for the phenomenon. Inspection of Fig. 7 indicates that under the best of circumstances, the retrieval of cells in outlet b was less than unity: based on the cell magnetophoretic mobility, the calculated maximum $F_b = 0.86$, whereas the experimentally measured maximum $F_b = 0.75$. The incomplete retrieval of the magnetic cells in outlet b was the result of the cell magnetophoretic mobility distribution, and the transport, rather than equilibrium, character of the continuous separation process. Conceivably, the retrieval of the magnetic cells could be increased by staging the separation process at a total flow rate for which there is negligible cell retention inside the channel, and at which the cell retrieval in an outlet b is close to the maximum.

The cell magnetophoretic mobility measurement by CTV and theoretical framework of the process by the SPLITT analysis, combined with the pulse injection studies provided us with a self-consistent model of the cell separation process in the QMS system. The correct prediction of the F_b maxima based on the cell mobility measurements convinced us of the utility of the concept of the magnetophoretic mobility, and the feasibility of separation of cell variables (mobility) from the system variables (magnetic force field strength). The observed, small systematic differences in the separation as predicted on the basis of cell mobility, and as measured by the pulse injection method, provide a point of departure for further studies of the mechanism of cell motion in the presence of viscous stresses and magnetic body forces. This and earlier studies (16,18,29) have provided us with a basis for design of a QMS system for the high volume, rapid isolation of hematopoietic progenitor cells from bone marrow, umbilical cord blood, and blood of patients mobilized for apheresis.

NOMENCLATURE

A	surface area under the elution peak
B	magnetic field (field intensity, field induction, or field flux density)
B_0	magnetic field at the outer cylinder inner wall (at $\rho = 1$)
d	transport lamina thickness
F_a, F_b, F_w	retrieval factor in outlet a, outlet b, Eq. (7), or the accumulation wall, Eq. (8), respectively
h	height of the flow channel
L	length of the QMS separation element

MARCEL DEKKER, INC.
270 Madison Avenue, New York, New York 10016

m	magnetophoretic mobility
N	cell number
N_a, N_b	total number of cells crossing the detector a or detector b, respectively
$Q = Q_{a'} + Q_{b'} = Q_a + Q_b$	Total flow rate
$Q_{a'}$	inlet flow rate (sample)
$Q_{b'}$	inlet flow rate (carrier fluid)
Q_a	outlet flow rate (depleted fraction)
Q_b	outlet flow rate (enriched fraction)
QMS	quadrupole magnet flow sorter
r	radial coordinate
r_o	radius of inner wall of the outside cylinder
r_i	radius of inner wall of the inside cylinder
r_s	flow splitter radius
r_{ISC}	inlet splitting cylinder radius
r_{OSC}	outer splitting cylinder radius
S_m	magnetic force field strength (a gradient of the magnetic energy density), Eq. (2)
u_m	radial particle velocity
V	volume
z	axial coordinate

Subscripts

a	QMS outlet port designation (depleted fraction)
b	QMS outlet port designation (magnetically enriched cell fraction)
a′	QMS inlet port designation (feed cell sample)
b′	QMS inlet port designation (carrier)
ISC	inlet splitting cylinder
OSC	outlet splitting cylinder

Greek Letters

ρ	r/r_o
μ_0	magnetic permeability of vacuum

ACKNOWLEDGMENTS

This study was supported by the grants from the NIH (R01 CA62349 to M.Z., R33 CA81662 to J.J.C.), the NSF (BES-9731059 to J.J.C. and M.Z.), and NATO ("Research and Development Grant" to M.H.). We thankfully acknowledge technical assistance of Mr. Boris Kligman.

REFERENCES

1. Todd, P.; Pretlow, T.G. Separation of Living Cells. In *Cell Separation Science and Technology*; Compala, D.S., Todd, P., Eds.; ACS Symposium Series 464, American Chemical Society: Washington, 1991, 1–24.
2. Hunt, V.H. Preparation of Lymphocytes and Accessory Cells. In *Lymphocytes: A Practical Approach*; Klaus, G.G.B., Ed.; IRL Press: Oxford, 1987; 1–34.
3. Lazarus, H.M. Hematopoietic Progenitor Cell Transplantation in Breast Cancer: Current Status and Future Directions. Cancer Investig. **1998**, *16*, 102–126.
4. Auditore-Hargreaves, K.; Heimfeld, S.; Berenson, R.J. Selection and Transplantation of Hematopoietic Stem and Progenitor Cells. Bioconjug. Chem. **1994**, *5*, 287–300.
5. Shapiro, H.M. *Practical Cytometry*; Wiley–Liss, Inc.: New York, 1995.
6. Takayasu, M.; Duske, N.; Ash, S.R.; Friedlaender, F.J. HGMS (High-Gradient Magnetic Separation) Studies of Blood Cell Behavior in Plasma. IEEE Trans. Mag. **1982**, *18*, 1520–1522.
7. Takayasu, M.; Kelland, D.R.; Minervini, J.V. Feasibility of Direct Magnetic Separation of White Cells and Plasma from Whole Blood. IEEE Trans. Appl. Supercond. **2000**, *10*, 927–930.
8. Watson, J.H.P. Magnetic Filtration. J. Appl. Phys. **1973**, *44*, 4209–4213.
9. Thomas, T.E.; Abraham, S.J.R.; Otter, A.J.; Blackmore, E.W.; Lansdorp, P.M. High Gradient Magnetic Separation of Cells on the Basis of Expression Levels of Cell Surface Antigens. J. Immunol. Methods **1992**, *154*, 245–252.
10. Ugelstad, J.; Stenstad, P.; Kilaas, L.; Prestvik, W.S.; Herje, R.; Berge, A.; Hornes, E. Monodisperse Magnetic Polymer Particles. Blood Purif. **1993**, *11*, 347–360.
11. Radbruch, A.; Mechtold, B.; Thiel, A.; Miltenyi, S.; Pflueger, E. High-Gradient Magnetic Sorting. Methods Cell Biol. **1994**, *42*, 387–403.
12. Zborowski, M.; Sun, L.; Moore, L.R.; Williams, P.S.; Chalmers, J.J. Continuous Cell Separation Using Novel Magnetic Quadrupole Flow Sorter. J. Magn. Magn. Mater. **1999**, *194*, 224–230.
13. Sun, L.; Zborowski, M.; Moore, L.R.; Chalmers, J.J. Continuous, Flow-Through Immunomagnetic Cell Sorting in a Quadrupole Field. Cytometry **1998**, *33*, 469–475.
14. Zborowski, M. Physics of Magnetic Cell Sorting. In *Scientific and Clinical Applications of Magnetic Microcarriers*; Häfeli, U., Schütt, W., Teller, J., Zborowski, M., Eds.; Plenum Press: New York, 1997; 205–231.
15. Liberti, P.A.; Feeley, B.P. Analytical- and Process-Scale Cell Separation with Bioreceptor Ferroflids and High Gradient Magnetic Separation. In *Cell*

MARCEL DEKKER, INC.
270 Madison Avenue, New York, New York 10016

Separation Science and Technology; Compala, D.S., Todd, P., Eds.; ACS Symposium Series 464, American Chemical Society: Washington, 1991, 268–288.

16. Hoyos, M.; Moore, L.R.; McCloskey, K.E.; Margel, S.; Chalmers, J.J.; Zborowski, M. Elution Profiles of Magnetic Particles Pulse-Injected into an Annular, SPLITT-Like Channel Inside a Quadrupole Magnetic Field. J. Chromatogr. A **2000**, *903*, 99–116.
17. McCloskey, K.E.; Zborowski, M.; Chalmers, J.J. Magnetophoretic Mobilities Correlate to Surface Antigen Binding Capacities. Cytometry **2000**, *40*, 307–315.
18. Williams, P.S.; Zborowski, M.; Chalmers, J.J. Flow Rate Optimization for the Quadrupole Magnetic Cell Sorter. Anal. Chem. **1999**, *71*, 3799–3807.
19. Hartig, R.; Hausman, M.; Schmitt, J.; Herrmann, D.B.J.; Riedmeiller, M.; Cremer, C. Preparative Continuous Separation of Biological Particles by Means of Free-Flow Magnetopheresis in a Free-Flow Electrophoresis Chamber. Electrophoresis **1992**, *13*, 674–676.
20. Winoto-Morbach, S.; Tchikov, V.; Mueller-Ruchholtz, W. Magnetophoresis I. Detection of Magnetically Labeled Cells. J. Clin. Lab. Anal. **1994**, *8*, 400–406.
21. Schuett, W.; Hashimoto, N.; Shimizu, M. Application of Cell Electrophoresis for Clinical Diagnosis. In *Cell Electrophoresis*; Bauer, J., Ed.; CRC Press, Inc.: Boca Raton, 1994; 255–266.
22. Moore, L.R.; Nakamura, M.; Margel, S.; Chalmers, J.J.; Zborowski, M. Magnetophoretic Mobility Determination of Monodispersed, Magnetic Microspheres by Cell Tracking Velocimetry. J. Biochem. Biophys. Methods **2000**, *44*, 115–130.
23. Nakamura, M.; Chalmers, J.J.; Lasky, L.; Zborowski, M. Theoretical and Experimental Analysis of the Accuracy and Reproducibility of Cell Tracking Velocimetry. Exp. Fluids **2001**, *30*, 371–380.
24. Chalmers, J.J.; Haam, S.; Zhao, Y.; McCloskey, K.; Moore, L.R.; Zborowski, M. Quantification of Cellular Properties from External Fields and Resulting Induced Velocity: Magnetic Susceptibility. Biotechnol. Bioeng. **1999**, *64*, 519–526.
25. Giddings, J.C. Field-Flow Fractionation: Analysis of Macromolecular, Colloidal, and Particulate Materials. Science **1993**, *260*, 1456–1465.
26. Sutherland, D.R.; Keating, A. The CD34 Antigen: Structure, Biology, and Potential Clinical Applications. J. Hematother. **1992**, *1*, 115–129.
27. Civin, C.I.; Gore, S.D. Antigenic Analysis of Hematopoiesis: A Review. J. Hematother. **1993**, *2*, 137–144.
28. Moore, L.R.; Zborowski, M.; Sun, L.; Chalmers, J.J. Lymphocyte Fractionation Using Immunomagnetic Colloid and Dipole Magnet Flow Sorter. J. Biochem. Biophys. Methods **1998**, *37*, 11–33.

MARCEL DEKKER, INC.
270 Madison Avenue, New York, New York 10016

29. Moore, L.R.; Rodriguez, A.; Williams, P.S.; McCloskey, K.; Bolwell, B.J.; Nakamura, M.; Chalmers, J.J.; Zborowski, M. Progenitor Cell Isolation with a High-Capacity Quadrupole Magnetic Flow Sorter. J. Magn. Magn. Mater. **2001**, *225*, 277–284.

Received November 2000
Revised July 2001

MARCEL DEKKER, INC.
270 Madison Avenue, New York, New York 10016

Request Permission or Order Reprints Instantly!